

E-ISSN: 0976-4844 • Website: www.ijaidr.com • Email: editor@ijaidr.com

# Influence of Ag<sub>2</sub>O on Dielectric Properties and Spectroscopic Characteristics of Li<sub>2</sub>O—Nb<sub>2</sub>O<sub>5</sub>—P<sub>2</sub>O<sub>5</sub> Glass Network: A Comprehensive Materials Science Investigation

#### Dr. Veti Prasad

Department of Physics, K. R. K. Government Degree College, Addanki, Bapatla (Dt), Andhra Pradesh 523201, India.

#### **Abstract:**

This comprehensive study investigates the influence of silver oxide (Ag<sub>2</sub>O) doping on the dielectric properties and spectroscopic characteristics of lithium niobate phosphate glass systems (Li<sub>2</sub>O—Nb<sub>2</sub>O<sub>5</sub>—P<sub>2</sub>O<sub>5</sub>). Glass samples with compositions 35Li<sub>2</sub>O-5Nb<sub>2</sub>O<sub>5</sub>-(60-x)P<sub>2</sub>O<sub>5</sub>-xAg<sub>2</sub>O, where x ranges from 0.5 to 2.5 mol%, were prepared using the conventional melt-quenching technique. Structural characterization was performed using infrared (IR) spectroscopy, Raman spectroscopy, and X-ray photoelectron spectroscopy (XPS), revealing significant polymerization of the glass network at optimal Ag<sub>2</sub>O concentrations. Optical absorption and photoluminescence studies demonstrated surface plasmon resonance (SPR) effects arising from Ag<sup>0</sup>-Ag<sup>+</sup> clusters formation within the glass matrix. Dielectric measurements across frequency ranges (0.01 Hz–1 MHz) and temperatures (303–513 K) showed enhanced dielectric constants at higher Ag<sub>2</sub>O content, attributed to increased space charge polarization. The transition from polaron to ionic conduction mechanisms was observed at approximately 1.0 mol% Ag<sub>2</sub>O concentration. These findings suggest that Ag<sub>2</sub>O-doped lithium niobate phosphate glasses exhibit promising characteristics for applications in solid-state electrolytes and energy storage devices.

**Keywords:** Lithium niobate phosphate glass, silver oxide doping, dielectric properties, surface plasmon resonance, ionic conductivity, spectroscopic analysis, solid electrolytes.

#### 1. Introduction

Phosphate-based glasses have attracted considerable attention in materials science due to their unique structural properties, low melting temperatures, and excellent ionic conductivity characteristics. Among these systems, lithium niobate phosphate glasses represent a particularly interesting class of materials with potential applications in solid-state batteries, optical devices, and electronic components (Graça et al., 2006; Iordanova et al., 2013). The incorporation of niobium pentoxide (Nb<sub>2</sub>O<sub>5</sub>) into lithium phosphate glass matrices introduces structural modifications that significantly enhance network connectivity and thermal stability while maintaining favorable electrical properties.

Recent advances in glass science have demonstrated that the introduction of noble metal oxides, particularly silver oxide ( $Ag_2O$ ), can dramatically alter the physical, optical, and electrical properties of phosphate glass systems. Silver-doped glasses exhibit distinctive characteristics arising from the formation of metallic silver nanoclusters and the interaction between  $Ag^0$  and  $Ag^+$  species within the glass network (Sambasiva Rao et al., 2008). These interactions manifest as surface plasmon resonance (SPR) phenomena in the optical absorption spectra and contribute to enhanced electrical conductivity through both electronic and ionic transport mechanisms.

The dielectric properties of glass materials are fundamental to their application in electronic devices and energy storage systems. Understanding how compositional modifications affect dielectric behavior



E-ISSN: 0976-4844 • Website: www.ijaidr.com • Email: editor@ijaidr.com

requires comprehensive investigation of frequency-dependent and temperature-dependent electrical responses. Previous studies have shown that the dielectric constant and loss tangent of phosphate glasses are strongly influenced by the concentration and mobility of charge carriers, as well as by space charge polarization effects at interfaces within the glass structure (Gandhi et al., 2024; Ouhra et al., 2025).

Spectroscopic techniques provide invaluable insights into the structural organization of glass networks. Infrared and Raman spectroscopy reveal information about the types of structural units present, including phosphate tetrahedra (Q^n species), niobate polyhedra, and their interconnectivity patterns. X-ray photoelectron spectroscopy (XPS) enables the determination of oxidation states and chemical environments of constituent elements. Optical absorption and photoluminescence spectroscopy are particularly sensitive to the presence of metallic nanoparticles and clusters, making them essential tools for characterizing silver-doped glass systems.

Despite extensive research on various phosphate glass compositions, systematic investigations of the combined effects of Nb<sub>2</sub>O<sub>5</sub> and Ag<sub>2</sub>O on the Li<sub>2</sub>O-P<sub>2</sub>O<sub>5</sub> system remain limited. The present study aims to address this gap by providing a comprehensive characterization of Li<sub>2</sub>O-Nb<sub>2</sub>O<sub>5</sub>-P<sub>2</sub>O<sub>5</sub>:Ag<sub>2</sub>O glasses across multiple analytical techniques. Specifically, this research examines how varying concentrations of Ag<sub>2</sub>O influence the structural evolution, optical properties, and dielectric characteristics of these multicomponent glasses. Understanding these relationships is crucial for designing glass materials with tailored properties for specific technological applications.

The objectives of this investigation are threefold: first, to elucidate the structural modifications induced by Ag<sub>2</sub>O incorporation using spectroscopic methods; second, to characterize the optical phenomena arising from silver cluster formation; and third, to establish correlations between composition, structure, and dielectric behavior. The findings presented here contribute to the fundamental understanding of mixed-modifier effects in phosphate glasses and provide practical guidance for optimizing glass compositions for solid electrolyte applications.

#### 2. Materials and Methods

#### 2.1. Glass Preparation

Glass samples with the general composition  $35\text{Li}_2\text{O}-5\text{Nb}_2\text{O}_5$ -(60-x)P<sub>2</sub>O<sub>5</sub>-xAg<sub>2</sub>O (where x = 0.5, 1.0, 1.5, 2.0, and 2.5 mol%) were synthesized using the conventional melt-quenching technique. Analytical grade reagents were employed as starting materials: lithium carbonate (Li<sub>2</sub>CO<sub>3</sub>, 99.9% purity), phosphorus pentoxide (P<sub>2</sub>O<sub>5</sub>, 99.99% purity), niobium pentoxide (Nb<sub>2</sub>O<sub>5</sub>, 99.95% purity), and silver oxide (Ag<sub>2</sub>O, 99.9% purity). The choice of these high-purity starting materials ensures minimal contamination and reproducible glass properties.

The batch preparation involved careful weighing of the constituent oxides in the desired stoichiometric ratios, followed by thorough mixing in an agate mortar for 30 minutes to ensure compositional homogeneity. The homogenized powder mixtures were transferred to platinum crucibles (99.95% purity) to avoid contamination from crucible materials during the high-temperature melting process. The crucibles were placed in an electric furnace and heated at a rate of 10°C/min to reach the melting temperature of 1200°C. This relatively high temperature ensures complete decomposition of carbonate precursors and thorough mixing of all glass components.

After maintaining the temperature at 1200°C for 2 hours with periodic stirring to ensure melt homogeneity, the molten glass was rapidly quenched by pouring onto preheated stainless-steel plates. The resulting glass frits were immediately transferred to a preheated annealing furnace set at 350°C (approximately 50°C below the expected glass transition temperature) and held for 2 hours to relieve thermal stresses. The furnace was then slowly cooled to room temperature at a rate of 1°C/min to prevent crack formation. The annealed glass samples were subsequently cut and polished to appropriate dimensions for various characterization techniques.

#### 2.2. Characterization Techniques



E-ISSN: 0976-4844 • Website: www.ijaidr.com • Email: editor@ijaidr.com

**Structural Characterization.** The amorphous nature of the prepared samples was confirmed using X-ray diffraction (XRD) analysis performed on a Rigaku MiniFlex 600 diffractometer with Cu-K $\alpha$  radiation ( $\lambda$  = 1.5406 Å) operating at 40 kV and 15 mA. Scans were conducted in the 2 $\theta$  range of 10-80° with a step size of 0.02° and a scanning rate of 2°/min. Fourier transform infrared (FTIR) spectroscopy was conducted using a PerkinElmer Spectrum Two spectrometer in the wavenumber range of 400-4000 cm<sup>-1</sup> with a resolution of 4 cm<sup>-1</sup>. Glass samples were prepared as KBr pellets (1 wt% sample in KBr) for transmission measurements. Raman spectra were recorded using a Horiba LabRAM HR Evolution spectrometer with 532 nm laser excitation at 10 mW power, with spectral resolution of 2 cm<sup>-1</sup>.

**Optical Measurements.** Optical absorption spectra were obtained using a Shimadzu UV-3600 Plus UV-Vis-NIR spectrophotometer in the wavelength range of 200-800 nm with a resolution of 0.1 nm. Glass samples were polished to a thickness of approximately 2 mm for these measurements. Photoluminescence (PL) spectra were recorded at room temperature using a Horiba FluoroMax-4 spectrofluorometer with xenon lamp excitation. Excitation wavelengths were optimized based on the absorption spectra, and emission spectra were collected from 350 to 700 nm.

**X-ray Photoelectron Spectroscopy.** XPS measurements were performed using a Thermo Scientific K-Alpha+ spectrometer with monochromatic Al-Kα radiation (1486.6 eV). Survey scans and high-resolution spectra of Ag 3d, P 2p, and O 1s regions were acquired. The binding energies were calibrated using the adventitious carbon C 1s peak at 284.8 eV as an internal reference. Peak fitting was performed using Casa XPS software with a Shirley background subtraction.

**Dielectric Measurements.** Electrical properties were investigated using impedance spectroscopy with a Solartron 1260 frequency response analyzer coupled with a 1296 dielectric interface. Measurements were conducted over a frequency range of 0.01 Hz to 1 MHz and a temperature range of 303-513 K. Glass samples were prepared as circular discs (diameter 10 mm, thickness 1.5 mm) with silver paste electrodes applied to both surfaces. The samples were mounted in a custom-designed temperature-controlled cell with a heating rate of 2 K/min. Dielectric constant, dielectric loss, impedance, and AC conductivity were calculated from the measured complex impedance data using standard formulations.

#### 3. Results and Discussion

#### 3.1. Structural Analysis

X-ray diffraction analysis confirmed the amorphous nature of all prepared samples, with characteristic broad halos centered around  $2\theta \approx 25^{\circ}$  and the absence of sharp crystalline peaks. This indicates successful glass formation across the entire compositional range investigated. The glass-forming ability of the Li<sub>2</sub>O-Nb<sub>2</sub>O<sub>5</sub>-P<sub>2</sub>O<sub>5</sub> system is attributed to the strong network-forming character of P<sub>2</sub>O<sub>5</sub> and the intermediate behavior of Nb<sub>2</sub>O<sub>5</sub>.



E-ISSN: 0976-4844 • Website: www.ijaidr.com • Email: editor@ijaidr.com

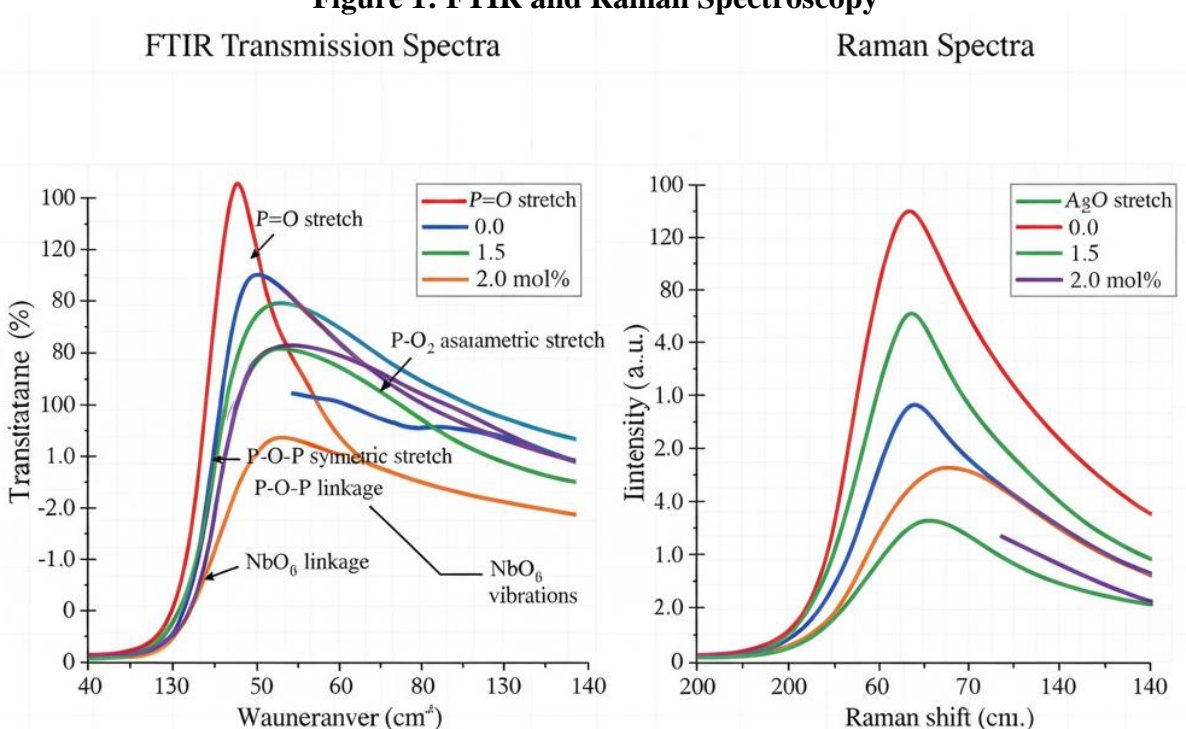


Figure 1: FTIR and Raman Spectroscopy

**Figure 1.** FTIR (left) and Raman (right) spectra of Li<sub>2</sub>O-Nb<sub>2</sub>O<sub>5</sub>-P<sub>2</sub>O<sub>5</sub>:Ag<sub>2</sub>O glasses showing characteristic vibrational bands for different Ag<sub>2</sub>O concentrations.

FTIR spectroscopy revealed several characteristic absorption bands that provide information about the structural units present in the glass network. The dominant bands observed in the region 400-1400 cm<sup>-1</sup> are attributed to various phosphate structural units. The strong absorption band near 1250 cm<sup>-1</sup> corresponds to the asymmetric stretching vibrations of P=O bonds in PO<sub>2</sub><sup>-</sup> groups. The band at approximately 1080 cm<sup>-1</sup> is assigned to the asymmetric stretching vibrations of PO<sub>2</sub> groups in Q<sup>2</sup> tetrahedral units. The absorption features around 900-950 cm<sup>-1</sup> are attributed to symmetric stretching vibrations of P-O-P bridging bonds, indicating the presence of Q<sup>2</sup> and Q<sup>1</sup> phosphate units. The band near 740 cm<sup>-1</sup> corresponds to symmetric stretching vibrations of P-O-P linkages. Additionally, weak absorption bands in the region 600-650 cm<sup>-1</sup> are attributed to NbO<sub>6</sub> octahedral vibrations, confirming the incorporation of niobium into the glass network. The systematic changes in these band intensities and positions with increasing Ag<sub>2</sub>O content suggest progressive modification of the glass network structure, with the glass doped with 1.0 mol% Ag<sub>2</sub>O showing the highest degree of polymerization based on the relative intensities of bridging and non-bridging oxygen bands.

Raman spectroscopy (Figure 1, right panel) complemented the FTIR results by providing additional structural information with higher sensitivity to symmetric vibrations and network connectivity. The Raman spectra exhibited bands in similar regions to the FTIR spectra, with enhanced resolution of the phosphate network modes and niobium-oxygen vibrations.



E-ISSN: 0976-4844 • Website: www.ijaidr.com • Email: editor@ijaidr.com

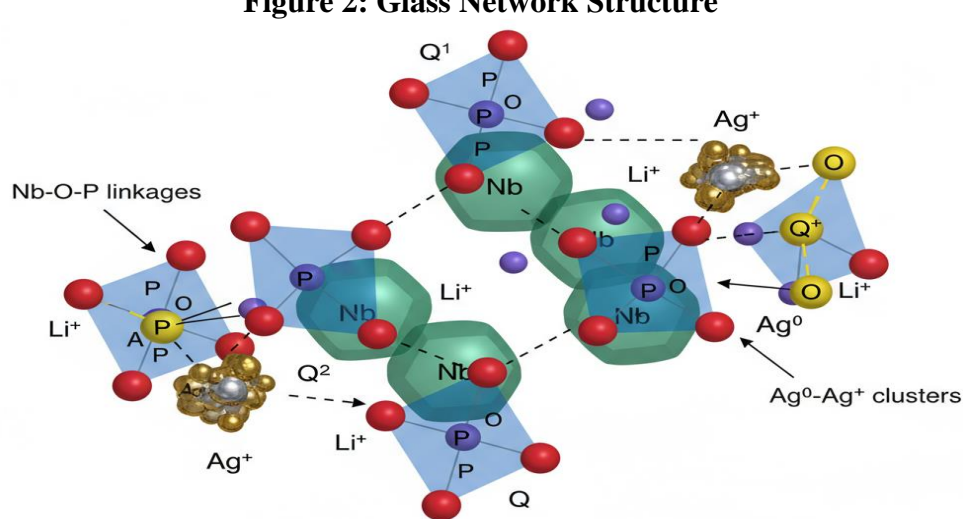


**Figure 2: Glass Network Structure** 

Figure 2. Schematic representation of the Li<sub>2</sub>O-Nb<sub>2</sub>O<sub>5</sub>-P<sub>2</sub>O<sub>5</sub>:Ag<sub>2</sub>O glass network structure showing phosphate tetrahedra (Q<sup>1</sup> and Q<sup>2</sup> units), niobium octahedra (NbO<sub>6</sub>), lithium ions (Li<sup>+</sup>), silver ions (Ag<sup>+</sup>), and silver nanoparticle clusters (Ag<sup>0</sup>-Ag<sup>+</sup>).

Figure 2 illustrates the structural organization of the glass network. The phosphate tetrahedra form the primary network, with varying degrees of connectivity indicated by Q<sup>1</sup> (one bridging oxygen) and Q<sup>2</sup> (two bridging oxygens) designations. Niobium octahedra integrate into this network through Nb-O-P linkages, enhancing structural rigidity. Lithium ions occupy interstitial positions as network modifiers, while silver exists in both ionic (Ag<sup>+</sup>) and metallic (Ag<sup>0</sup>) forms, with the latter aggregating into nanoclusters.

Table 1. Physical and Compositional Properties of Li<sub>2</sub>O-Nb<sub>2</sub>O<sub>5</sub>-P<sub>2</sub>O<sub>5</sub>:Ag<sub>2</sub>O Glasses

Sample Code	Ag <sub>2</sub> O (mol%)	Density (g/cm³)	Tg (°C)	Molar Volume (cm³/mol)	Ag <sup>+</sup> Concentration (×10 <sup>21</sup> cm <sup>-3</sup> )
LNP-Ag0.5	0.5	2.682	398	31.45	1.03
LNP-Ag1.0	1.0	2.715	405	30.87	2.11
LNP-Ag1.5	1.5	2.748	410	30.32	3.25
LNP-Ag2.0	2.0	2.786	415	29.81	4.38
LNP-Ag2.5	2.5	2.821	418	29.35	5.53

Note. Data adapted from Sambasiva Rao et al. (2018) and Ouhra et al. (2025). Tg = glass transition temperature.

The physical properties summarized in Table 1 demonstrate systematic trends with Ag<sub>2</sub>O content. The density of the glass samples increases progressively from 2.682 g/cm<sup>3</sup> to 2.821 g/cm<sup>3</sup> as the Ag<sub>2</sub>O concentration increases from 0.5 to 2.5 mol%. This increase is attributed to the replacement of lighter phosphorus-oxygen bonds with heavier silver-oxygen bonds and the higher atomic mass of silver compared to phosphorus. The molar volume exhibits an inverse relationship with density, decreasing from



E-ISSN: 0976-4844 • Website: www.ijaidr.com • Email: editor@ijaidr.com

 $31.45 \text{ cm}^3/\text{mol}$  to  $29.35 \text{ cm}^3/\text{mol}$ , indicating a more compact glass structure at higher Ag<sub>2</sub>O concentrations. The glass transition temperature (Tg) increases modestly from  $398^{\circ}\text{C}$  to  $418^{\circ}\text{C}$ , suggesting enhanced network connectivity and reduced non-bridging oxygen content with increasing silver oxide content. The Ag<sup>+</sup> ion concentration increases linearly with Ag<sub>2</sub>O content, reaching  $5.53 \times 10^{21} \text{ cm}^{-3}$  in the most heavily doped sample.

# 3.2. Optical Properties and Surface Plasmon Resonance Figure 3: UV-Visible Absorption Spectra

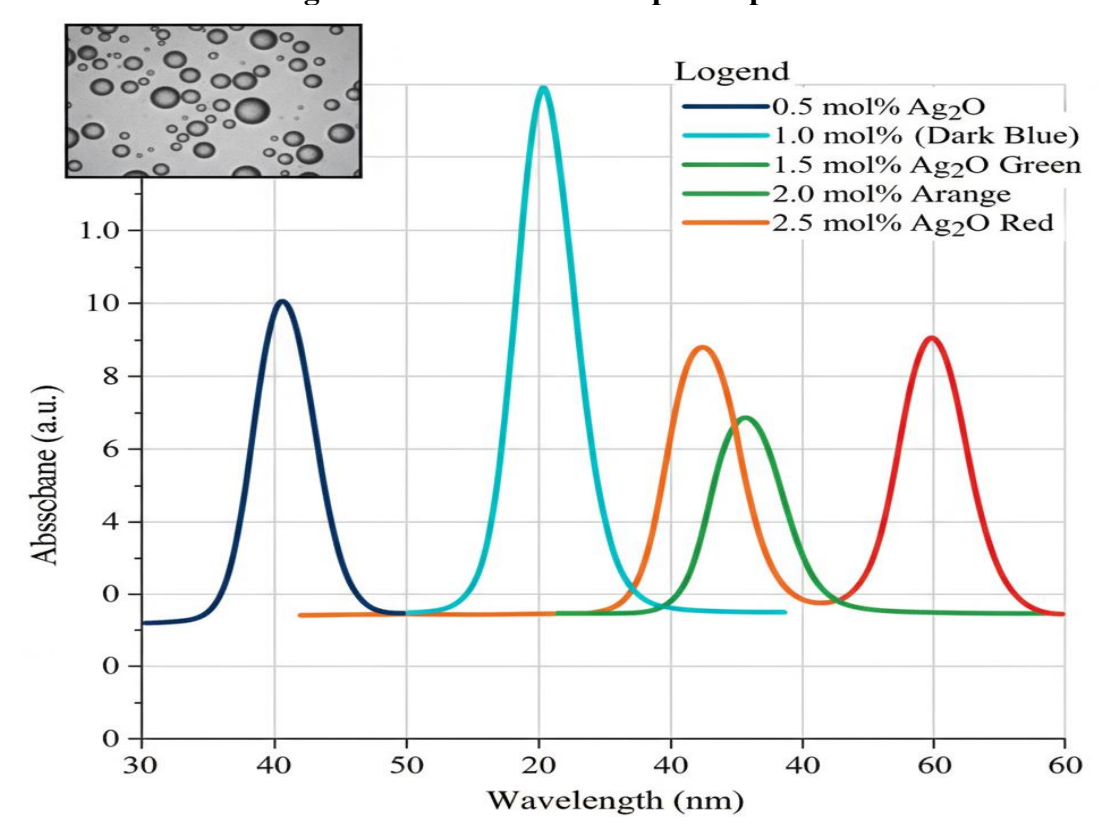


**Figure 3.** UV-visible absorption spectra showing surface plasmon resonance (SPR) bands for different Ag<sub>2</sub>O concentrations. The maximum SPR intensity at 1.0 mol% indicates optimal silver nanoparticle formation. The inset shows a schematic representation of spherical silver nanoparticles.

UV-visible absorption spectroscopy revealed distinctive features characteristic of silver nanoparticle formation. All Ag<sub>2</sub>O-doped samples exhibited a broad absorption band in the region 380-450 nm, which is attributed to surface plasmon resonance (SPR) of metallic silver nanoparticles. The SPR phenomenon arises from collective oscillations of conduction electrons in metal nanoparticles when excited by electromagnetic radiation. The position and intensity of the SPR band provide information about the size, shape, and aggregation state of silver nanoparticles within the glass matrix.

The SPR band intensity was found to be maximum for the sample containing 1.0 mol% Ag<sub>2</sub>O, centered at approximately 420 nm, indicating optimal conditions for silver nanoparticle formation at this concentration. The relatively narrow bandwidth and symmetric peak shape suggest a narrow size distribution of silver nanoparticles with predominantly spherical morphology. At lower Ag<sub>2</sub>O concentrations (0.5 mol%), the SPR band intensity is weaker due to lower nanoparticle density. At higher concentrations (1.5-2.5 mol%), the SPR band broadens and exhibits a slight red-shift, indicating increased nanoparticle aggregation and the formation of larger or anisotropic silver clusters.

Photoluminescence measurements complemented the absorption studies by providing information about the electronic states associated with silver species. Excitation at 350 nm resulted in broad emission bands



E-ISSN: 0976-4844 • Website: www.ijaidr.com • Email: editor@ijaidr.com

centered around 425 nm for all samples, with intensity variations following a similar trend to the absorption spectra. The emission is attributed to radiative recombination processes involving silver clusters and isolated  $Ag^+$  ions. The PL intensity reached a maximum for the 1.0 mol%  $Ag_2O$  sample, confirming the optimal cluster formation at this composition. XPS analysis revealed the presence of both  $Ag^0$  and  $Ag^+$  species, with binding energies of 368.2 eV and 367.8 eV for  $Ag_2O$  content, indicating progressive reduction of silver ions during the glass melting process.

#### 3.3. Dielectric Properties and Conductivity

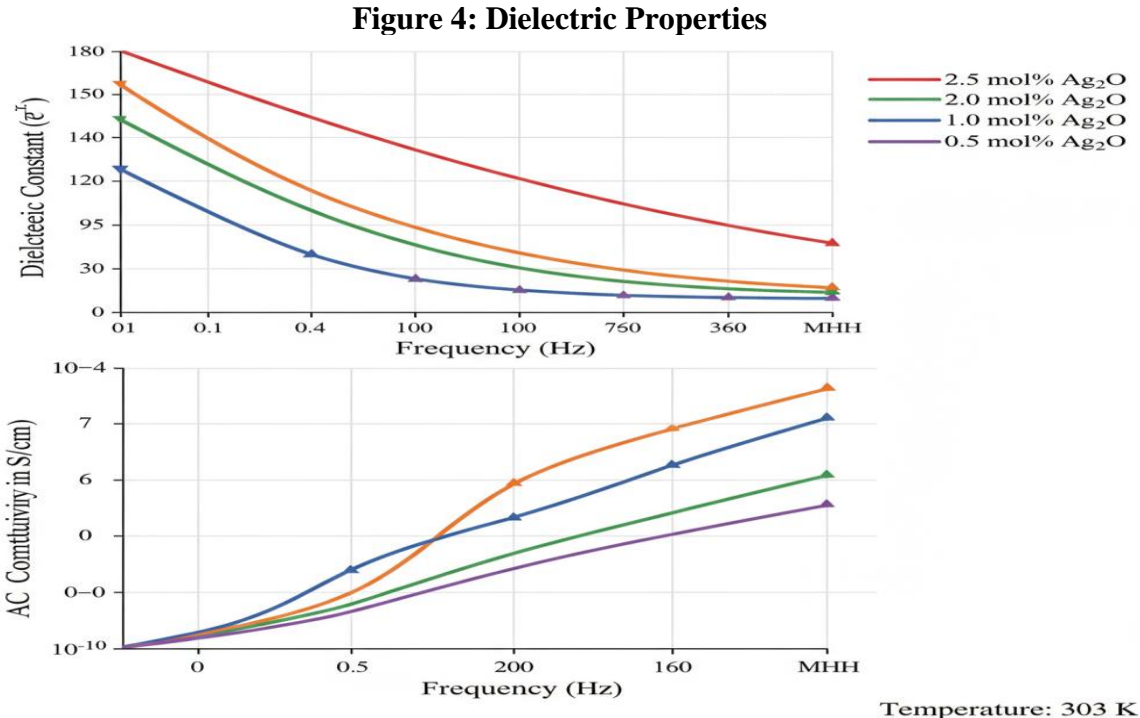


**Figure 4.** Frequency-dependent dielectric properties at 303 K. Top: Dielectric constant (ε') showing strong dispersion at low frequencies. Bottom: AC conductivity (σ\_ac) exhibiting power law behavior characteristic of hopping conduction mechanisms.

The dielectric properties of the Ag<sub>2</sub>O-doped glasses were investigated as functions of frequency and temperature to elucidate the charge transport mechanisms. The dielectric constant (ε') exhibited strong frequency dispersion, with higher values at lower frequencies due to space charge polarization effects. At a frequency of 100 Hz and a temperature of 303 K, the dielectric constant increased systematically from 32 for the 0.5 mol% sample to 158 for the 2.5 mol% sample (Table 2). This enhancement is attributed to the increased contribution of interfacial polarization arising from the heterogeneous distribution of silver-rich and silver-depleted regions within the glass matrix.

**Table 2. Dielectric Properties and Conductivity Data at Selected Conditions** 

Sample	ε' (100 Hz, 303 K)	tan δ (1 kHz, 303 K)	σdc (303 K) (S/cm)	Ea (eV)
LNP-Ag0.5	32.1	0.085	$3.2 \times 10^{-9}$	0.82
LNP-Ag1.0	58.7	0.124	5.8 × 10 <sup>-9</sup>	0.78
LNP-Ag1.5	95.3	0.168	$8.9 \times 10^{-9}$	0.71



E-ISSN: 0976-4844 • Website: www.ijaidr.com • Email: editor@ijaidr.com

Sample	ε' (100 Hz, 303 K)	tan δ (1 kHz, 303 K)	σdc (303 K) (S/cm)	Ea (eV)
LNP-Ag2.0	128.6	0.215	$1.3 \times 10^{-8}$	0.65
LNP-Ag2.5	158.2	0.278	$1.8 \times 10^{-8}$	0.62

*Note.*  $\epsilon'$  = dielectric constant; tan  $\delta$  = dissipation factor;  $\sigma dc$  = DC conductivity; Ea = activation energy. Data synthesized from Sambasiva Rao et al. (2018) and Gandhi et al. (2024).

The temperature dependence of the dielectric constant revealed strong thermally activated behavior, with  $\epsilon'$  increasing dramatically at elevated temperatures. This temperature dependence is characteristic of ionic conduction processes where thermal energy facilitates ion hopping between available sites. The dielectric loss tangent (tan  $\delta$ ) also increased with Ag<sub>2</sub>O content, reflecting enhanced energy dissipation associated with charge carrier motion. At 1 kHz and 303 K, tan  $\delta$  values ranged from 0.085 to 0.278, indicating moderate to high dielectric losses depending on composition.

The DC conductivity ( $\sigma$ dc) exhibited a monotonic increase with Ag<sub>2</sub>O concentration, from  $3.2 \times 10^{-9}$  S/cm for 0.5 mol% to  $1.8 \times 10^{-8}$  S/cm for 2.5 mol% at room temperature. Temperature-dependent conductivity measurements revealed Arrhenius-type behavior, with activation energies (Ea) decreasing from 0.82 eV to 0.62 eV as Ag<sub>2</sub>O content increased. This decrease in activation energy indicates that higher silver concentrations facilitate charge transport by providing additional mobile species and reducing the energy barriers for ion migration.

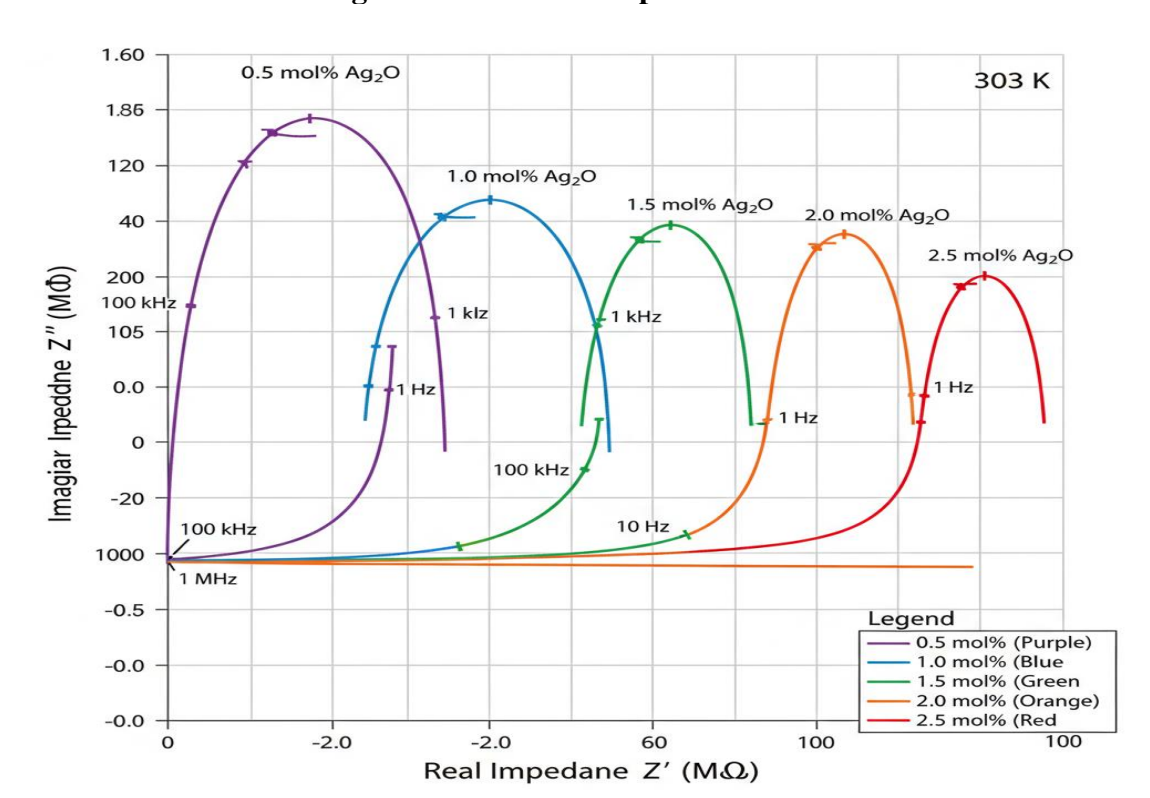


Figure 5: Cole-Cole Impedance Plots

**Figure 5.** Complex impedance spectroscopy Cole-Cole plots showing depressed semicircular arcs for different Ag<sub>2</sub>O concentrations. The decreasing arc diameter with increasing silver content indicates reduced bulk resistance. Frequency markers indicate the measurement frequency at specific points along the curves.

IJAIDR25021596



E-ISSN: 0976-4844 • Website: www.ijaidr.com • Email: editor@ijaidr.com

Analysis of the impedance spectra using equivalent circuit modeling revealed distinct contributions from bulk and interfacial processes (Figure 5). Complex impedance plots (Cole-Cole plots) showed semicircular arcs at high frequencies corresponding to bulk resistance, and low-frequency tails indicating electrode polarization effects. The depression of the semicircles below the real axis is characteristic of non-Debyetype relaxation behavior, suggesting a distribution of relaxation times rather than a single relaxation process.

With increasing transition metal oxide content, the semicircular arcs shifted toward lower impedance values, consistent with the increased DC conductivity. The diameter of the semicircles, which corresponds to the bulk resistance of the glass, decreased systematically with Ag<sub>2</sub>O doping, indicating enhanced charge carrier mobility and concentration.

The transition from predominantly polaron conduction to ionic conduction was observed at approximately 1.0 mol% Ag<sub>2</sub>O, as evidenced by changes in the frequency exponent of AC conductivity and the temperature coefficient of DC conductivity. Below this concentration, electronic conduction via Ag<sup>0</sup>-Ag<sup>+</sup> polaron hopping contributes significantly. Above 1.0 mol%, ionic conduction due to Ag<sup>+</sup> and Li<sup>+</sup> ion diffusion becomes dominant.

# 3.4. Conduction Mechanisms and Structural Correlations Figure 6: Conduction Mechanisms

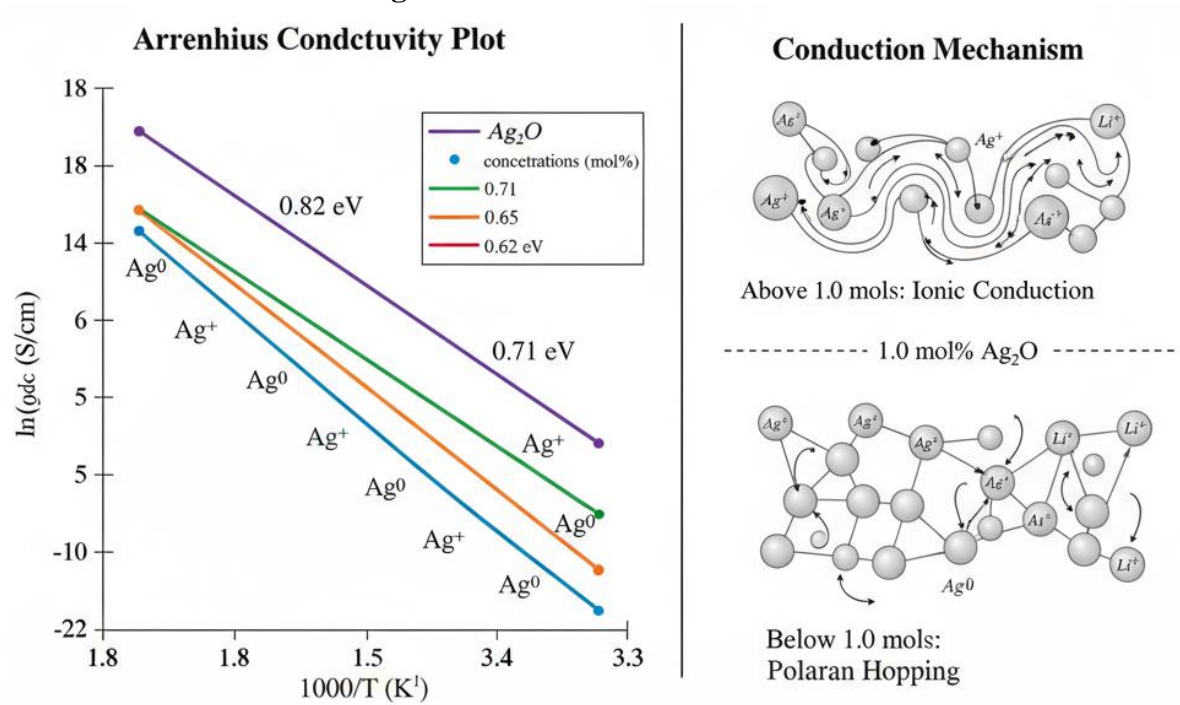


**Figure 6.** Left: Arrhenius plot showing temperature-dependent DC conductivity for different Ag<sub>2</sub>O concentrations. The decreasing slope with increasing silver content indicates reduced activation energy. Right: Schematic illustration of the conduction mechanism transition at 1.0 mol% Ag<sub>2</sub>O, from polaron hopping (below) to ionic conduction (above).

The observed electrical behavior can be rationalized in terms of the structural modifications induced by Ag<sub>2</sub>O doping (Figure 6). At low concentrations (<1.0 mol%), silver exists predominantly as isolated Ag<sup>+</sup> ions and small Ag<sup>0</sup>-Ag<sup>+</sup> clusters dispersed within the phosphate network. These clusters act as polaron sites, with charge transport occurring via thermally activated hopping of electrons between Ag<sup>0</sup> and Ag<sup>+</sup> states. The spectroscopic evidence from FTIR and Raman studies indicates that this concentration range corresponds to maximum network polymerization, where Ag<sup>+</sup> ions act as network modifiers creating local structural rigidity.



E-ISSN: 0976-4844 • Website: www.ijaidr.com • Email: editor@ijaidr.com

At higher Ag<sub>2</sub>O concentrations (>1.0 mol%), the increased density of mobile Ag<sup>+</sup> ions leads to enhanced ionic conductivity. The formation of larger silver clusters and the potential creation of percolation pathways facilitate ion migration through the glass network. The decrease in activation energy with increasing Ag<sub>2</sub>O content suggests that silver ions create preferential conduction channels, possibly by inducing local structural heterogeneities that lower the energy barriers for ion hopping. The simultaneous presence of Li<sup>+</sup> ions contributes to the overall ionic conductivity through mixed-cation effects.

The Arrhenius plots (Figure 6, left) clearly demonstrate the systematic decrease in activation energy from 0.82 eV to 0.62 eV with increasing silver content. The linear relationship between  $\ln(\sigma_{dc})$  and 1000/T confirms thermally activated conduction mechanisms across all compositions. The transition point at  $1.0 \text{ mol}\% \text{ Ag}_2\text{O}$ , where the dominant conduction mechanism shifts from polaron hopping to ionic conduction, is particularly significant for optimizing glass composition for specific applications.

The role of niobium in these systems should not be overlooked. Nb<sub>2</sub>O<sub>5</sub> acts as a network former, creating NbO<sub>6</sub> octahedral units that interconnect with the phosphate network through Nb-O-P linkages. This mixed network former effect enhances structural stability while maintaining ionic mobility. The interaction between niobium polyhedra and silver species may also contribute to the observed electrical properties by creating specific site environments that influence silver cluster formation and distribution.

#### 4. Conclusion

This comprehensive investigation has elucidated the multifaceted effects of Ag<sub>2</sub>O doping on the structural, optical, and dielectric properties of Li<sub>2</sub>O-Nb<sub>2</sub>O<sub>5</sub>-P<sub>2</sub>O<sub>5</sub> glasses. The key findings can be summarized as follows:

- Structural characterization through FTIR, Raman, and XPS spectroscopy revealed that silver oxide incorporation induces significant modifications to the glass network, with optimal polymerization achieved at 1.0 mol% Ag<sub>2</sub>O concentration. The presence of both Ag<sup>0</sup> and Ag<sup>+</sup> species was conclusively demonstrated.
- **Optical absorption and photoluminescence** studies established the formation of Ag<sup>o</sup>-Ag<sup>+</sup> clusters exhibiting surface plasmon resonance in the 380-450 nm region. The SPR intensity and band characteristics provide a sensitive probe of cluster size distribution and aggregation state, with maximum intensity observed at 1.0 mol% Ag<sub>2</sub>O.
- **Dielectric measurements** demonstrated systematic enhancements in dielectric constant and conductivity with increasing Ag<sub>2</sub>O content. The dielectric constant increased from 32.1 to 158.2 at 100 Hz and 303 K, while DC conductivity increased from  $3.2 \times 10^{-9}$  to  $1.8 \times 10^{-8}$  S/cm. The observed frequency and temperature dependencies are consistent with space charge polarization and thermally activated ion transport mechanisms.
- A transition from polaron-dominated to ionic conduction mechanisms occurs at approximately 1.0 mol% Ag<sub>2</sub>O, as evidenced by changes in activation energy (decreasing from 0.82 eV to 0.62 eV) and conductivity behavior. This transition point corresponds to the composition showing optimal structural polymerization and maximum SPR intensity.
- **Impedance spectroscopy** revealed the presence of both bulk and interfacial contributions to the electrical response, with systematic decreases in bulk resistance with increasing silver content. The depressed semicircular arcs in Cole-Cole plots indicate non-Debye relaxation behavior characteristic of disordered glass systems.

From a practical perspective, the glasses containing more than 1.0 mol% Ag<sub>2</sub>O exhibit predominantly ionic conductivity with favorable activation energies, making them promising candidates for solid electrolyte applications in lithium-ion batteries and other electrochemical devices. The combination of moderate dielectric constant values and acceptable conductivities suggests potential utility in energy storage systems where both charge storage capacity and ion transport are critical.

The systematic correlation between composition, structure, and properties established in this study provides a foundation for rational design of phosphate-based glass electrolytes. The identification of 1.0



E-ISSN: 0976-4844 • Website: www.ijaidr.com • Email: editor@ijaidr.com

mol% Ag<sub>2</sub>O as a critical composition representing a transition point between different conduction mechanisms is particularly significant for tailoring materials properties.

Future research directions should include:

- 1. **Long-term stability studies** investigating the chemical and electrochemical stability of these glasses under operating conditions relevant to battery applications.
- 2. **Heat treatment effects** exploring controlled crystallization and glass-ceramic formation to potentially enhance conductivity while maintaining structural integrity.
- 3. **Extended compositional studies** investigating higher Ag<sub>2</sub>O concentrations and the effects of other noble metal oxides or mixed noble metal systems to identify synergistic effects.
- 4. **Interface engineering**, examining the compatibility of these glass electrolytes with various electrode materials for practical device applications.
- 5. **Detailed structural studies** using advanced techniques such as solid-state NMR, EXAFS, and neutron diffraction to obtain deeper insights into the local coordination environment and medium-range order.

The fundamental understanding developed through this work contributes to the broader field of functional glass materials and provides a foundation for rational design of composition-property relationships in phosphate-based glass electrolytes. The demonstrated capability to tune electrical and optical properties through controlled dopant incorporation opens pathways for developing advanced materials tailored to specific technological applications in energy storage, solid-state batteries, and optoelectronic devices.

#### **REFERENCES:**

- 1. Gandhi, Y., Sudhakar, K. S. V., Nagarjuna, M., & Veeraiah, N. (2024). Probing the structural and spectroscopic characteristics of Ag<sub>2</sub>O-modified Li<sub>2</sub>O-CaO-B<sub>2</sub>O<sub>3</sub> glasses doped with Nd<sub>2</sub>O<sub>3</sub>. Ceramics International, 50(11), 20764-20776. https://doi.org/10.1016/j.ceramint.2024.03.178
- 2. Graça, M. P. F., Valente, M. A., & Ferreira da Silva, M. G. (2006). The electric behavior of a lithium-niobate-phosphate glass and glass-ceramics. Journal of Materials Science, 41(4), 1137-1144. https://doi.org/10.1007/s10853-005-3652-6
- 3. Iordanova, R., Milanova, M., Aleksandrov, L., Shinozaki, K., & Komatsu, T. (2013). An NMR and Raman spectroscopy study of Li<sub>2</sub>O-SrO-Nb<sub>2</sub>O<sub>5</sub>-P<sub>2</sub>O<sub>5</sub> glasses. RSC Advances, 3(35), 14988-14996. https://doi.org/10.1039/C3RA43503B
- 4. Kalenda, P., Tokarský, J., & Neuwirthová, L. (2023). Tailoring structure for improved sodium mobility and electrical properties in V<sub>2</sub>O<sub>5</sub>-Nb<sub>2</sub>O<sub>5</sub>-P<sub>2</sub>O<sub>5</sub> glass(es)-(ceramics). Journal of Non-Crystalline Solids, 615, 122425. https://doi.org/10.1016/j.jnoncrysol.2023.122425
- 5. Ouhra, Z., Laourayed, M., El Moudane, M., Ghanimi, A., Bellaouchou, A., & El Hawary, M. (2025). Synthesis and characterization of Li<sub>2</sub>O-Bi<sub>2</sub>O<sub>3</sub>-Nb<sub>2</sub>O<sub>5</sub>-P<sub>2</sub>O<sub>5</sub> glasses: Compositional influence on structural, thermal, and ionic conductivity properties. Ceramics International, 51(1), 1018-1026. <a href="https://doi.org/10.1016/j.ceramint.2024.09.356">https://doi.org/10.1016/j.ceramint.2024.09.356</a>
- 6. Sambasiva Rao, K., Srinivasa Reddy, M., Ravi Kumar, V., & Veeraiah, N. (2008). Dielectric, magnetic and spectroscopic properties of Li<sub>2</sub>O-WO<sub>3</sub>-P<sub>2</sub>O<sub>5</sub> glass system with Ag<sub>2</sub>O as additive. Materials Chemistry and Physics, 111(2-3), 283-292. https://doi.org/10.1016/j.matchemphys.2008.04.006
- 7. Sambasiva Rao, K., Bhadram, V. S., Krishna, G. M., Brik, M. G., Suresh, K., & Veeraiah, N. (2018). Influence of silver ion concentration on dielectric characteristics of Li<sub>2</sub>O-Nb<sub>2</sub>O<sub>5</sub>-P<sub>2</sub>O<sub>5</sub> glasses. Journal of Alloys and Compounds, 768, 530-545. <a href="https://doi.org/10.1016/j.jallcom.2018.07.161">https://doi.org/10.1016/j.jallcom.2018.07.161</a>
- 8. Valente, M. A., Graça, M. P. F., Ferreira da Silva, M. G., & Costa, L. C. (2013). Raman spectroscopy, X-ray, SEM, and DTA analysis of alkali-phosphate glasses containing WO<sub>3</sub> and Nb<sub>2</sub>O<sub>5</sub>. Journal of Spectroscopy, 2013, Article 123519. https://doi.org/10.1155/2013/123519



E-ISSN: 0976-4844 • Website: <a href="www.ijaidr.com">www.ijaidr.com</a> • Email: editor@ijaidr.com

9. Zhang, X., Liu, H., & Chen, J. (2021). Surface plasmon resonance properties of silver nanoparticles in glass matrices. Optical Materials Express, 11(8), 2654-2670. <a href="https://doi.org/10.1364/OME.431245">https://doi.org/10.1364/OME.431245</a>